Decay pathways of superexcited states of nitrous oxide*

Lin Mei(林 梅)[a], Liu Ya-Wei(刘亚伟)[a], Zhong Zhi-Ping(钟志萍)[b], and Zhu Lin-Fan(朱林繁)[a]†

[a] *Hefei National Laboratory for Physical Sciences at Microscale, Department of Modern Physics, University of Science and Technology of China, Hefei* 230026, *China*

[b] *School of Physical Sciences, University of the Chinese Academy of Sciences, Beijing* 100049, *China*

(Received 3 November 2013; revised manuscript received 3 January 2014; published online 25 March 2014)

The ionization and ionic dissociation of the superexcited state of N_2O are studied by using electron energy loss spectroscopy and positive ion time-of-flight mass spectroscopy at different momentum transfers; that is, 0 and 0.23 a.u. (atomic unit) . The transitions at 13.8 eV and 14.0 eV are reassigned as $3p\pi(000)$ and $3p\sigma(000)$ converging to $A^2\Sigma^+$, respectively. The competition between the main decay pathways of superexcited states at different momentum transfers is revealed. It is found that $3d\sigma$ converging to $C^2\Sigma^+$ mainly decays into N_2O^+ while $4d\sigma$ can decay into both N_2O^+ and NO^+.

Keywords: ionization continuum, superexcited states, decay channel, nitrous oxide

PACS: 34.80.Gs, 32.70.Cs, 33.80.Eh, 33.20.Ni **DOI:** 10.1088/1674-1056/23/5/053403

1. Introduction

As intermediates in atmospheric chemistry, N_2O and N_2O^+ are well known and have received increasing attention in recent years, which is one reason for the existence of a substantial literature on N_2O photochemistry. Nitrous oxide, which was documented in the Kyoto protocol,[1,2] is one of six greenhouse gases, and its photolytic product NO can destroy stratospheric O_3. Therefore, the research of dissociation and ionization processes of nitrous oxide by photoabsorption or electron impact is crucial to atmospheric physics and circumstance science. In addition, as a simple polyatomic molecule, triatomic and linear N_2O has attracted the interest of quantum chemistry theorists because of the difficulty and accessibility of theoretical calculations.[3] Therefore, from a purely scientific viewpoint, N_2O is a good candidate to test the quantum chemical method.

Nitrous oxide has 22 electrons, and its ground-state electronic configuration can be written as $(1\sigma)^2(2\sigma)^2(3\sigma)^2(4\sigma)^2(5\sigma)^2(6\sigma)^2(1\pi)^4(7\sigma)^2(2\pi)^4$. Extensive experimental works have been conducted to study the superexcited states of N_2O, most of which were carried out by: photoabsorption,[4–6] photoionization,[7–10] photoelectron energy spectroscopy,[11–14] photoionization mass spectroscopy,[7,15,16] photon-induced fluorescence,[9,17–19] and photoelectron-photoion coincidence spectroscopy.[20–22] Among these, the cross sections of the structured ionization region and their decay pathways have been investigated by Refs. [5], [7]–[9], and [17], and the competition between autoionization and predissociation of Rydberg states were clearly revealed.[9] Furthermore, the Rydberg states converging to different ionic states are assigned and the mechanism of photoionization was studied.[7]

By now, most of the experimental works investigating the superexcited states of N_2O have been performed by using optical methods, in which the squared momentum transfer is close to zero. In recent years, the electron impact method has also been used to investigate the cross sections of the structured ionization region and the superexcited states of N_2O,[23–25]; however, most of these works were carried out by Brion's group using the dipole (e, e+ion) method, in which momentum transfer dependence behaviors of different superexcited states cannot be observed because the momentum transfer is also close to zero. There have been few investigations[26–28] of the momentum transfer dependence behaviors of the structured ionization region of N_2O, and these works recorded the electron energy loss spectra (EELSs) or double differential cross sections at different scattering angles with different incident electron energies, some different features of dipole-forbidden superexcited states stand out. However, the momentum transfer dependence behaviours of decay pathways of the superexcited states or ionization continuum of N_2O have not been investigated by any experiment.

In another respect, some theoretical works have been carried out to investigate the photoabsorption and photoionization cross sections of Rydberg states.[29–32] Among them, references [30] and [31] calculated the photoabsorption and photoionization cross sections for the ionization continuum using the molecular-adapted quantum defect orbital method (MQDO). Reference [32] reported the optical oscillator strength of Rydberg series of N_2O in a similar way, and

*Project supported by the National Natural Science Foundation of China (Grants Nos. U1332204, 11274291, and 11074299), the National Basic Research Program of China (Grant No. 2010CB923301), the Specialized Research Fund for the Doctoral Program of Higher Education of China, and the Fundamental Research Funds for the Central Universities of Ministry of Education of China.

†Corresponding author. E-mail: lfzhu@ustc.edu.cn

© 2014 Chinese Physical Society and IOP Publishing Ltd

when compared with previous theoretical work their calculated results are more consistent with the experimental observations. However, these works are still in the stage of qualitative or half quantitative description. There is no theoretical work of the decay processes of the superexcited states or ionization continuum and the momentum transfer dependence behavior of N_2O.

In this paper, we have investigated the ionization and ionic dissociation in the decay of the structured ionization region by the method of electron-ion coincidence from the ionization threshold to 30 eV. The generalized oscillator strength density (GOSD) and the partial GOSD of fragment ions were measured at the scattering angles of 0° and 2°. In our spectra, the decay pathways of the superexcited states converging to $A^2\Sigma^+$ and $C^2\Sigma^+$ at different momentum transfers were measured.

2. Experimental method

In the present work, the electron-energy-loss spectrometer was used, which has been described in detail in our previous works.[33–35] Briefly, we obtained the EELS by measuring the scattering electron counts at special energy loss. We acquire the decay information of definite superexcited states or the ionization continuum by measuring ions and the scattered electrons coincidently. The EELS is absolutized according to the double differential cross section obtained in the same energy region previously.[36] It is then transferred into the generalized oscillator strength density spectra. It is well known that the relative ionization efficiency of a molecule generally approaches a constant and it can be normalized to a unit when the energy loss is above 20 eV.[37] Therefore, the relative partial GOSDs of the fragments can be absolutized by the same factor.

In the present experiment, the incident electron energy was set at 2.5 keV with an energy resolution of about 80 meV. The mass resolution of time of flight mass spectrometer (TOFMS) in this work was about 53 a.m.u. All the spectra were recorded at a pressure of 1×10^{-3} Pa with the background pressure in the vacuum chamber being 5×10^{-5} Pa. The electron energy loss spectra and ion yield spectra of N_2O were recorded at 0° and 2°, and the energy loss regions of the spectra were set at 10.04–30.52 eV. The true zero angle was determined by the symmetry of the angular distribution of intensity of the transition of the $1^1S\rightarrow2^1P$ transition of helium at 21.218 eV. The energy scales of the measured spectra are also calibrated by referencing to this transition.

The total experimental error of GOSD or partial GOSD was about 20%–40%, which mainly came from the statistical counts, the ionization efficiency, as well as the normalization procedure of double differential cross section.

3. Results and discussion

Figure 1 shows the GOSD of the structured ionization region 12.0–22.0 eV of N_2O at 0° ($K^2 = 0$ a.u.) and 2° ($K^2 = 0.23$ a.u.). The superexcited states in Fig. 1 are assigned according to Refs. [7] and [8] and the present work, herein $\tilde{X}^2\Pi$, $\tilde{A}^2\Sigma^+$, $\tilde{B}^2\Pi$, and $\tilde{C}^2\Sigma^+$ represent the ionization thresholds of N_2O, which correspond to the ionic states where an electron is knocked out from the orbits of 2π, 7σ, 1π, and 6σ, respectively.

The peaks at 13.8 eV and 14.0 eV are shown as the up-arrows in Fig. 1. These two transitions are assigned as $3p\sigma(000)$ and $3p\pi(000)$ converging to $\tilde{A}^2\Sigma^+$ by Ref. [7], respectively. From Fig. 1, it can be observed that the peak at 13.8 eV is obvious at small momentum transfer, but its intensity decreases as the momentum transfer grows larger, the peak becomes hardly observable at a scattering angle of 2°. This is a typical behavior of the dipole-allowed transition. However, the peak at 14.0 eV is very small at 0° and stands out at 2°, which means that the intensity of this peak becomes larger with larger momentum transfer. This is a typical behavior of the dipole-forbidden transition. The aforementioned momentum transfer dependence behaviors of dipole-allowed transition and dipole-forbidden transition have been observed in atoms[38–41] and molecules.[36,42,43] Considering that the dipole-forbidden transitions in the united atom model may become dipole-allowed in the separated atom model, they can be observed in the photoabsorption spectrum,[7,8] such as the transition of $X^1\Sigma^+ \rightarrow B^1\Sigma^+$ of CO.[42] The intensity of this kind of transition (e.g., the peak at 14.0 eV of N_2O and the transition of $X^1\Sigma^+ \rightarrow B^1\Sigma^+$ of CO) is weak in photoabsorption spectrum. In the electron collision experiments it increases with the increase of momentum transfer in the small momentum transfer region, just like the peak at 14.0 eV that is shown in Fig. 1. Because the transitions at 13.8 eV and 14.0 eV are both excitations from 7σ electron, we believe that the transition at 13.8 eV corresponds to $3p\pi(000)$ while the transition at 14.0 eV corresponds to $3p\sigma(000)$ which is different from the assignments of these two transitions in Ref. [7].

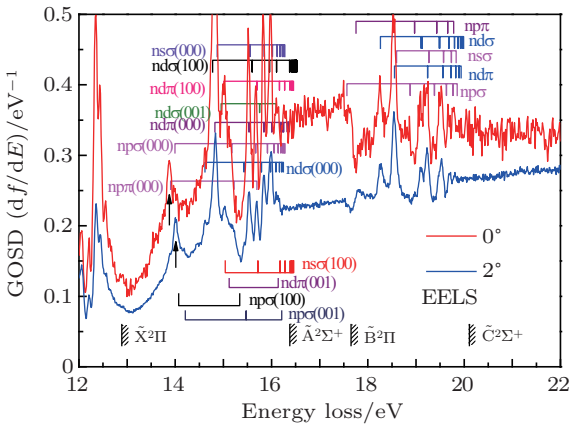


Fig. 1. The GOSD in 12.0–22.0 eV of N_2O at 0° and 2°.

Our assignment of these two transitions is based on their momentum transfer dependence behaviors, as mentioned above. In addition, for N_2O, the 7σ electron corresponds to $2p\sigma$, the transition of $2p\sigma \rightarrow 3p\sigma$ is dipole-forbidden from the viewpoint of united atom model while it is dipole-allowed from the viewpoint of the separated atom model. Consequently, its intensity is very weak in the photoabsorption spectrum and increases as momentum transfer increases in the small momentum transfer region, which accords to the situation of the peak at 14.0 eV that is shown in Fig. 1. The transition of $7\sigma \rightarrow 3p\pi$ is a typical electric dipole-allowed transition, its momentum transfer dependence behavior is consistent with the condition of the peak at 13.8 eV. Furthermore, the ground state of N_2O is $X\,^1\Sigma^+$ and the spin-allowed transitions from the ground state consists of $(7\sigma)^{-1}3p\sigma\,^1\Sigma^+$ and $(7\sigma)^{-1}3p\pi\,^1\Pi$. From the viewpoint of the molecular point group, the transition of $^1\Sigma^+ \rightarrow {}^1\,\Pi$ is electric dipole- and quadrupole-allowed, while the transition of $^1\Sigma^+ \rightarrow {}^1\,\Sigma^+$ is electric monopole-, dipole- and quadrupole-allowed. Compared with $(7\sigma)^{-1}3p\pi\,^1\Pi$, which includes electric dipole and quadrupole compositions, $(7\sigma)^{-1}3p\sigma\,^1\Sigma^+$ includes monopole, dipole, and quadrupole compositions. The momentum transfer dependence behavior of the transition of atoms reveals that the intensity of monopole transition is often larger than the intensity of quadrupole transition with the same configuration.[39–41] Therefore, $3p\sigma$ should be more obvious at large momentum transfer. In addition, the calculation shows that the lowest unoccupied orbital of N_2O is 3π followed by 8σ,[44] while 3π and 8σ correspond to $3p\pi$ and $3p\sigma$, respectively. Consequently, the energy level of $3p\sigma$ is likely to be higher than the energy level of $3p\pi$, which is consistent with our assignment. Therefore, we assign the peak at 13.8 eV as $3p\pi(000)$ while the peak at 14.0 eV as $3p\sigma(000)$.

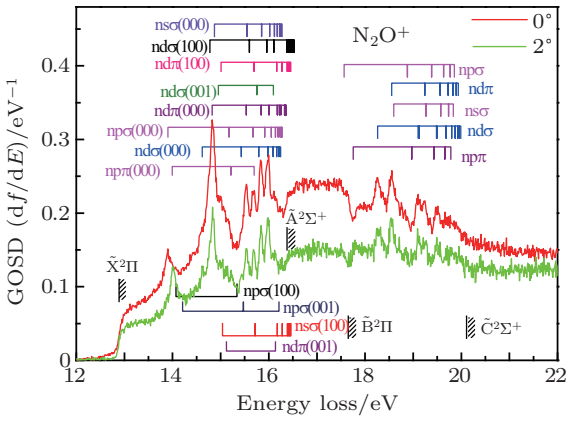


Fig. 2. The partial GOSD of N_2O^+ in 12.0–22.0 eV of N_2O at 0° and 2°.

Figures 2 and 3 show the partial GOSDs of N_2O^+ and NO^+ at 0° and 2°. It can be seen that the Rydberg series converging to $\tilde{A}^2\Sigma^+$ dominantly decays into N_2O^+. For the Rydberg series converging to $\tilde{C}^2\Sigma^+$, $3p\sigma$, $3p\pi$, and $3d\sigma$ are invisible in the spectrum of NO^+ while they are obvious in the spectrum of N_2O^+, which indicates that they mainly decay into N_2O^+. However, $4d\sigma$ is obvious in the spectrum of NO^+, which is different from the behavior of $3d\sigma$. $3d\pi$ decays both into N_2O^+ and NO^+. Because of the limited energy resolution and the poor statistical counts, the decay information of other superexcited states converging to $\tilde{C}^2\Sigma^+$ cannot be obtained.

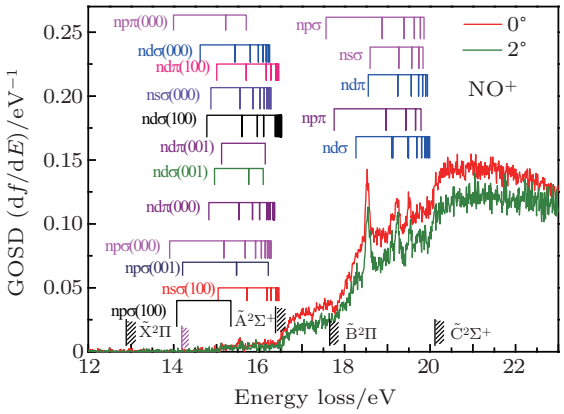


Fig. 3. The partial GOSD of NO^+ in 12.0–23.0 eV of N_2O at 0° and 2°.

Figures 4, 5, and 6 show the partial GOSDs of N_2^+, N^+, and O^+ at 0° and 2°. We notice that the partial GOSDs of N_2^+, N^+, and O^+ change a little at different momentum transfers, while the ones of N_2O^+ and NO^+ have obvious variation. However, we cannot give an explanation about this phenomenon. In Fig. 6, the broad ridge in 15.29–18.70 eV is assigned as the ionic dissociation of $N_2O^+ \rightarrow O^+ + N_2$.[7] Reference [20] indicates that the dissociation channel is $O^+(^4S_u) + N_2(X^1\Sigma_g^+)$ and the dissociation limit is 15.29 eV. However, the lower electronic states of N_2O^+ are $\tilde{X}^2\Pi$ and $\tilde{A}^2\Sigma^+$, cannot dissociate into $O^+(^4S_u) + N_2(X^1\Sigma_g^+)$ because they are spin-forbidden. Reference [45] indicates that the ionic dissociation process is through the bent ionic state $1^4A''$ of N_2O^+ which is from the high vibrational state $X^2\Pi$.

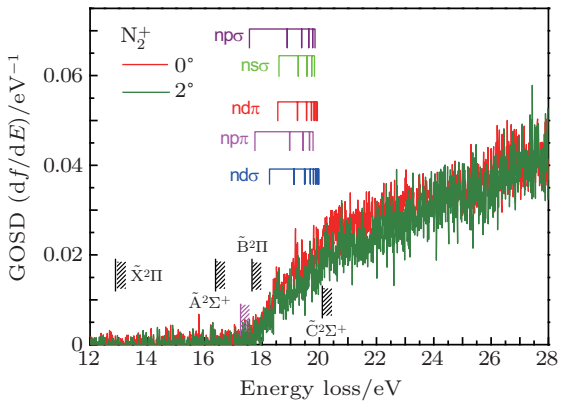


Fig. 4. The partial GOSD of N_2^+ in 12.0–23.0 eV of N_2O at 0° and 2°.

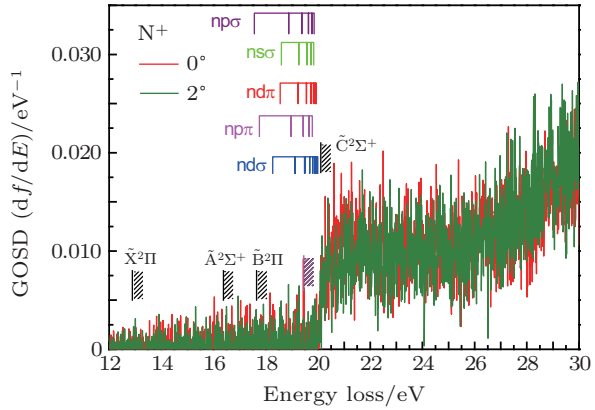


Fig. 5. The partial GOSD of N^+ in 12.0–23.0 eV of N_2O at 0° and 2°.

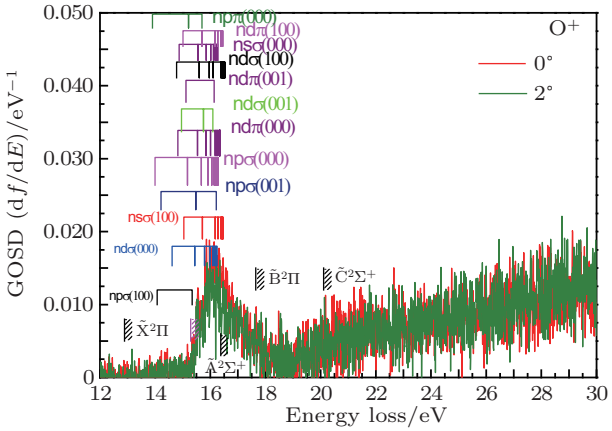


Fig. 6. The partial GOSD of O^+ in 12.0–23.0 eV of N_2O at 0° and 2°.

4. Summary

The electron energy loss spectra and the partial GOSDs of ionic fragments at the scattering angles of 0° and 2° of N_2O have been measured at an electron impact energy of 2500 eV with an energy resolution of 80 meV. The Rydberg states 3pσ(000) and 3pπ(000) are reassigned based on their momentum transfer dependence behaviors. According to the partial GOSD of ionic fragments, the behavior of the decay pathways of superexcited states of nitrous oxide at different momentum transfers are revealed. It is found that 3dσ converging to $\tilde{C}^2\Sigma^+$ mainly decays into N_2O^+ while 4dσ can decay into N_2O^+ and NO^+.

References

[1] Yung Y L, Wang W C and Lacis A A 1976 *Geophys. Res. Lett.* **3** 619
[2] Crutzen P J 1971 *J. Geophys. Res.* **76** 7311
[3] Dand M N, Balint-Kurti G G and Brown A 2005 *J. Chem. Phys.* **122** 054305
[4] Cook G R, Metzger P H and Ogawa M 1968 *J. Opt. Soc. Am.* **58** 129
[5] Lee L C, Carlson R W, Judge D L and Ogawa M 1973 *J. Quant. Spectrosc. Radiat. Transfer.* **13** 1023
[6] Cole B E and Dexter R N 1978 *J. Phys. B* **11** 1011
[7] Berkowitz J and Eland J H D 1977 *J. Chem. Phys.* **67** 2740
[8] Shaw D A, Holland D M P, Macdonald M A, Hopkirk A, Hayes M A and Mcsweeney S M 1992 *Chem. Phys.* **163** 387
[9] Shaw D A and Holland D M P 2008 *J. Phys. B* **41** 145103
[10] Baer T, Guyon P M, Nenner I, Fouhaille A T, Botter R, Ferreira L F A, and Govers T R 1979 *J. Chem. Phys.* **70** 1585
[11] Dehmer P M, Dehmer J L and Chupka W A 1980 *J. Chem. Phys.* **73** 126
[12] Sokell E, Wills A A and Comer J 1996 *J. Phys. B* **29** 3417
[13] Sokell E, Wills A A, Comer J and Hammond P 1997 *J. Phys. B* **30** 2635
[14] Truesdale C M, Southworth S, Kobrin P H, Lindle D W and Shirley D A 1983 *J. Chem. Phys.* **78** 7117
[15] Szarka M G and Wallace S C 1991 *J. Chem. Phys.* **95** 2336
[16] Masuoka T and Mitani S 1989 *J. Chem. Phys.* **90** 2651
[17] Shaw D A and Holland D M P 2008 *Chem. Phys.* **352** 217
[18] Ukai M, Kameta K, Machida S, Kouchi N, Hatano Y and Tanaka K 1994 *J. Chem. Phys.* **101** 5473
[19] Machida S, Ukai M, Kitajima M, Kameta K, Kouchi N, Hatano Y, Hayaishi T and Ito K 1997 *J. Phys. Chem. A* **101** 656
[20] Kinmond E, Eland J H D and Karlsson L 1999 *Int. J. Mass Spetrometry* **185** 437
[21] Richardviard M, Atabek O, Dutuit O and Guyon P M 1990 *J. Chem. Phys.* **93** 8881
[22] Nenner I, Guyon P, Baer T and Govers T R 1980 *J. Chem. Phys.* **72** 6587
[23] Hitchcock A P, Brion C E and van Der Wiel M J 1980 *Chem. Phys.* **45** 461
[24] Chan W F, Cooper G and Brion C E 1994 *Chem. Phys.* **180** 77
[25] Wang Y X, Zhu L F, Liu X J, Jiang X M, Yuan Z S, Yang T and Xu K Z 2001 *Chin. J. Chem. Phys.* **14** 33 (in Chinese)
[26] Lee J S 1977 *J. Chem. Phys.* **67** 3998
[27] England K, Reddish T and Comer J 1988 *Chem. Phys.* **119** 435
[28] Dillon M A, DeMille D and Spence D 1987 *J. Elect. Spectrosc. Relat. Phenom.* **42** 67
[29] Kilcoyne D A L, Nordholm S and Hush N S 1986 *Chem. Phys.* **107** 225
[30] Velasco A M, Bustos E, Martin I and Lavin C 2001 *Int. J. Quant. Chem.* **84** 70
[31] Martin I, Velasco A M, Lavin C, Olalla E and Bustos E 2001 *Int. J. Quant. Chem.* **85** 345
[32] Bustos E, Velasco A M, Martin I and Lavin C 2002 *J. Phys. Chem. A* **106** 35
[33] Lin M, Liu Y W, Zhong Z P and Zhu L F 2013 *Chin. Phys. B* **22** 023404
[34] Wu S L, Zhong Z P, Feng R F, Xing S L, Yang B X and Xu K Z 1995 *Phys. Rev. A* **51** 4494
[35] Liu X J, Zhu L F, Jiang X M, Yuan Z S and Cai B 2001 *Rev. Sci. Instrum.* **72** 3357
[36] Wang Y Y, Sun J M and Zhu L F 2010 *J. Chem. Phys.* **132** 124301
[37] Gallagher J W, Brion C E, Samson J A R and Langhoff P W 1988 *J. Phys. Chem. Ref. Data.* **17** 9
[38] Liu X J, Zhu L F, Yuan Z S, Li W B, Cheng H D, Huang Y P, Zhong Z P, Xu K Z and Li J M 2003 *Phys. Rev. Lett.* **91** 193203
[39] Cheng H D, Zhu L F, Yuan Z S, Liu X J, Sun J M, Jiang W C and Xu K Z 2005 *Phys. Rev. A* **72** 012715
[40] Zhu L F, Yuan H, Jiang W C, Zhang F X, Yuan Z S, Cheng H D and Xu K Z 2007 *Phys. Rev. A* **75** 032701
[41] Li W B, Zhu L F, Liu X J, Yuan Z S, Sun J M, Cheng H D, Zhong Z P and Xu K Z 2003 *Phys. Rev. A* **67** 062708
[42] Zhong Z P, Feng R F, Xu K Z, Wu S L, Zhu L F, Zhang X J, Ji Q and Shi Q C 1997 *Phys. Rev. A* **55** 1799
[43] Fan L L, Zhong Z P, Zhu L F, Liu X J, Yuan Z S, Sun J M and Xu K Z 2005 *Phys. Rev. A* **71** 032704
[44] Chutjian A and Segal G A 1972 *J. Chem. Phys.* **57** 3069
[45] Hopper D G 1978 *J. Am. Chem. Soc.* **100** 1019